

# TSWV modulates sex ratio in the western flower thrips, *Frankliniella occidentalis*, by down-regulating a FSCB-like gene

**Min Tao**

Chinese Academy of Agricultural Sciences

**Yanran Wan**

Chinese Academy of Agricultural Sciences

**Xiaobin Zheng**

Chinese Academy of Agricultural Sciences

**Kanghua Qian**

Chinese Academy of Agricultural Sciences

**Baoyun Xu**

Chinese Academy of Agricultural Sciences

**Youjun Zhang**

Chinese Academy of Agricultural Sciences

**Xuguo Zhou**

University of Kentucky

**Qingjun Wu** (✉ [wuqingjun@caas.cn](mailto:wuqingjun@caas.cn))

Chinese Academy of Agricultural Sciences

---

## Research Article

**Keywords:** *Frankliniella occidentalis*, TSWV, sex ratio, FoFSCB-like, male sterility

**Posted Date:** April 19th, 2022

**DOI:** <https://doi.org/10.21203/rs.3.rs-1540449/v1>

**License:**  This work is licensed under a Creative Commons Attribution 4.0 International License.

[Read Full License](#)

---

## Abstract

Plant viruses can facilitate their transmission by modulating sex ratios of their insect vectors. Previously, we found that exposure to tomato spotted wilt orthotospovirus (TSWV) in the western flower thrips, *Frankliniella occidentalis*, led to a male-biased sex ratio in the offspring. TSWV, a generalist pathogen with a broad host range, is transmitted primarily by *F. occidentalis* in a circulative-propagative manner. Here, we integrated proteomic tools with nanoparticle-mediated RNAi to comprehensively investigate the genetic basis underlying the shift in vector's sex ratio induced by virus. Proteomic analysis showed 104 differentially expressed proteins between *F. occidentalis* adult males with and without TSWV. The expression level of the fiber sheath CABYR-binding-like (FSCB) protein, namely FoFSCB-like, a sperm-specific protein associated with sperm capacitation and motility was decreased by 46%. The predicted FoFSCB-like protein include 10 classic Pro-X-X-Pro motifs and 42 phosphorylation sites, which are key features for sperm capacitation. The relative expression of *FoFSCB-like* was gradually increased alongside the developmental stages and peaked at the pupal stage. After exposed to TSWV, *FoFSCB-like* expression was substantially down-regulated. RNAi substantially suppressed *FoFSCB-like* expression and led to a significant male bias in the offspring. This study not only advances our understanding of virus-vector interactions, but also identifies a potential target for the genetic management of *F. occidentalis*, the primary vector of TSWV, by manipulating male fertility.

## Key Message

- Exposure of thrips to TSWV leads to a male-biased sex ratio in the offspring.
- Proteomic analysis revealed 104 differentially expressed proteins between male *F. occidentalis* with and without TSWV.
- *FoFSCB-like* expression was substantially down-regulated in *F. occidentalis* carrying TSWV.
- Nanoparticle-mediated RNAi significantly suppressed *FoFSCB-like* expression and led to a significant increase in the male offspring.
- Down-regulation of *FoFSCB-like* is responsible for the male-biased sex ratio.

## Introduction

Insects are the most important vectors of many devastating plant viruses (Gilbertson et al. 2015; Rotenberg et al. 2015), and research has demonstrated a strong win-win relationship between viruses and their insect vectors (Blanc and Michalakis 2016; Oliver and Whitfield 2016). This has increased the difficulty of controlling both viruses and insect pests. Many case studies reported that viruses can manipulate biochemical substances in their insect hosts, thereby enhancing insect adaptation to altered environments and promoting virus transmission (Ghosh et al. 2021; Stafford et al. 2011). For instance, the activation of heat shock protein (HSP) by southern rice black-streaked dwarf virus (SRBSDV) promotes the adaptation of the vector *Sogatella furcifera* to high temperature (Yu et al. 2021). In another example, tomato yellow leaf curl virus (TYLCV) can enter the ovary of female whiteflies, where its coat

protein interacts with vitellogenin (Vg), thus increasing both whitefly fecundity and the transovarial transmission of TYLCV (Wei et al. 2017). Such mutually beneficial relationships increase the prevalence and persistence of both viruses and vectors (Whitfield et al. 2015).

Tomato spotted wilt orthotospovirus (TSWV) belonging to the genus *Orthotospovirus* of the Bunyavirales family Tospoviridae, is one of the most destructive plant viruses (Scholthof et al. 2011). TSWV has caused substantial damage to agricultural crops worldwide (Gilbertson et al. 2015; Rotenberg et al. 2015; Whitfield et al. 2015). The transmission of TSWV in nature mainly depends on thrips and especially on the western flower thrips, *Frankliniella occidentalis* (Pergande). In addition to vectoring TSWV, the *F. occidentalis* alone is a serious pest of horticultural crops worldwide (Riley et al. 2011). Many studies indicate that TSWV has substantial effects on *F. occidentalis* biology and behavior, i.e. TSWV increases *F. occidentalis* fecundity and lifespan and alters its feeding and oviposition preferences (Ogada et al. 2016; Oliver and Whitfield 2016; Rotenberg et al. 2015; Wan et al. 2020a; Whitfield et al. 2015; Ziegler-Graff 2020). These effects benefit both *F. occidentalis* and TSWV. Interestingly, Wan et al. (2020a) found that exposure to TSWV altered the sex ratio of *F. occidentalis* offspring. Changes in the sex ratio of insects caused by viruses have also been documented for the wasp *Pteromalus puparum* (Linnaeus) when exposed to the virus PPNSRV-1 (Wang et al. 2017). More recently, Fujita et al. (2020) reported that Osugoroshi viruses can cause a shift in the sex ratio of the moth *Homona magnanima* (Diakonoff). Although the effects of viruses on the sex ratios of their vector insects have been well documented, the molecular basis for these effects is poorly understood.

Bisexual reproduction, in which a male provides sperm to combine with an egg and a female produces a fertilized egg, is the most common form of insect reproduction. In the process, the integrity of the flagellum, the main structure responsible for sperm motility, is required for normal sperm function (Krueger and Moritz 2021; Lehti and Sironen 2016; Li et al. 2010; Li et al. 2011; Liu et al. 2011; Nakamura et al. 2013; Young et al. 2016; Zhang et al. 2016). Evidence from mammals suggests that a defect in the flagellar structure often causes the loss of sperm motility, thereby inducing male sterility (Baccetti et al. 2005; Fiedler et al. 2013; Liu et al. 2011; Miki et al. 2002; Torres-Badia et al. 2021; Xu et al. 2020; Young et al. 2016; Zhang et al. 2016). Fiber sheath CABYR-binding protein (FSCB), an important sperm-specific protein, was first discovered in the fibrous sheath of mouse flagella in 2007 (Li et al. 2007). The FSCB protein in male mice has an important role in sperm capacitation by increasing  $\text{Ca}^{2+}$  concentration and tyrosine phosphorylation (Liu et al. 2011; Zhang et al. 2015). In addition, knockout of FSCB along with its binding partners ROPN1 and CABYR resulted in significant abnormalities in flagellum morphology and sperm motility in male mice (Li et al. 2011; Zhang et al. 2016). The results suggest that FSCB is essential for maintenance of male fertility through sperm capacitation and motility in mammals (Li et al. 2007; Liu et al. 2011; Zhang et al. 2016). To date, FSCB has been reported in mice, rats, and humans; only gene annotation information has been reported for insects such as *Aedes aegypti*, *Drosophila melanogaster*, *Bactrocera dorsalis*, etc. The role of FSCB in insects is poorly understood.

*Frankliniella occidentalis* has a haplodiploid genetic system, in which females are produced from fertilized diploid eggs, while males are produced from unfertilized haploid eggs (Adam et al. 2017; Bondy

and Hunter 2019). In nature, *F. occidentalis* are female-biased (Akinyemi 2018). We previously reported that TSWV-infected male *F. occidentalis* mated to normal females led to a shift in the sex ratio of offspring toward males(Wan et al. 2020a). The increase of male individuals among *F. occidentalis* offspring indicated that females produced more unfertilized eggs, that is, TSWV could change the sex ratio of offspring by influencing males. However, the mechanism by which TSWV regulates the sex ratio of *F. occidentalis* progeny remains unclear. Sterile insect technology (SIT) is a species-specific method of controlling target pests by releasing artificially sterilized insects that interfere with the mating between males and females. Zheng et al. (2019) used low-dose irradiation to produce large-scale sterile *Aedes albopictus* males to suppress field populations and thereby control the spread of mosquito-borne viruses such as dengue virus. The Mediterranean fruit fly, *Ceratitis capitata*, is a destructive fruit and vegetable pest causing extensive losses to citrus growers in Spain. Pla et al. (2021) applied SIT to control *C. capitata* and to improve the quality of citrus fruit while reducing the use of pesticide. SIT is an environmentally friendly pest control method and has become an important part of integrated pest management.

The basis of male sterility technology is the generation of non-viable sperm. Previously, our transcriptomic sequencing revealed that a gene annotated as *FSCB-like* was significantly down-regulated in *F. occidentalis* males infected with TSWV. Considering its role in sperm function, we hypothesized that down-regulation of *FSCB-like* can shift the offspring sex ratio toward males in *F. occidentalis*. To test this hypothesis, we 1) carried out comparative proteomic analysis of *F. occidentalis* males with and without TSWV to determine the effects of TSWV on the reproduction-related proteins; 2) identified and cloned *FoFSCB-like* genome sequence to understand its structural features; and finally 3) functionally characterized *FoFSCB-like* using nanomaterial-mediated RNA interference (RNAi).

## Materials And Methods

### *Frankliniella occidentalis* maintenance and TSWV acquisition

A virus-free *F. occidentalis* colony was isolated from an indoor strain that had been kept in our laboratory for nearly 20 years. Thrips were fed with fresh bean pods and were kept in glass jars in a climate chamber at  $26 \pm 1^\circ\text{C}$ , with 70 % relative humidity and a 16L: 8D photoperiod as described by Wan et al. (2020a). TSWV isolate TSWV-YN was maintained on *Datura stramonium* plants by thrips transmission. Young *D. stramonium* plants were mechanically inoculated with TSWV, and TSWV infection was confirmed 2 weeks later by double-antibody sandwich enzyme-linked immunosorbent assay (DAS-ELISA) using a purchased kit (Agdia Incorporated. Elkhart, Indiana, USA) and following the manufacturer's instructions. DAS-ELISA-positive plants were used for virus acquisition by newly hatched *F. occidentalis* nymphs (Wan et al. 2020b).The TSWV-infected plants were placed in an incubator at  $22 \pm 1^\circ\text{C}$  with 80 % relative humidity and a 16L: 8D photoperiod.

### Obtaining male thrips with and without TSWV

The large number of male thrips used in this study were obtained from arrhenotokous parthenogenesis of virgin females. Approximately 500 adult thrips (mixed sex) were placed in a glass rearing jar and allowed to lay eggs on fresh bean pods for 48 h. The bean pods with eggs were placed in another glass jar and reared to the pupal stage with fresh bean pods provided as needed. Pupae were transferred into a 1.5 mL centrifuge tube (one pupa per tube) using a fine paint brush. The sex of the newly emerged adults was determined by microscopic examination. All newly emerged virgin females were placed in a new glass jar and fed with fresh bean pods. Newly hatched 1<sup>st</sup>-instar nymphs (< 6 h) were collected and placed in a 15-cm-diameter petri dish. Half of the nymphs were reared on TSWV-infected *D. stramonium* leaves, and these were regarded as the TSWV infected group or TSWV (+); the other half was reared on healthy *D. stramonium* leaves, and these served as the control group or TSWV (-).

### Proteomic analysis

Approximately 400 1-day-old males were collected from TSWV (+) and TSWV (-) groups and were rapidly frozen in liquid nitrogen after being placed in 1.5 mL RNase-free centrifuge tubes. Five cohorts were separately collected from each group as five biological replicates. For the TSWV (+) group, the TSWV acquisition rate was detected by using qRT-PCR (Wan et al. 2020b). Only cohorts with an acquisition rate > 90 % were used for subsequent proteomic assays. The samples were suspended in lysis buffer (1 % SDS, 8 M urea) that included an appropriate protease inhibitor. The concentration of protein supernatant was determined by using the Pierce Bicinchoninic acid Protein Assay Kit (Thermo, USA). The samples were dissolved in 0.5 M tetraethylammonium bromide (TEAB) (Applied Biosystems, Milan, Italy). One unit of tandem mass tag (TMT) reagent was then thawed and reconstituted in 50 µL of acetonitrile. After they were tagged for 2 h at 37°C, all samples were pooled, desalting, and vacuum-dried (Jia et al. 2018; Zhong et al. 2019). Peptides were first separated with a gradient of eluent (phase A: 5 mM ammonium hydroxide solution containing 20 % acetonitrile, pH 10; phase B: 80 % acetonitrile, pH 10) by ACQUITY Ultra Performance liquid chromatography (UPLC) (Waters, USA) with an ACQUITY UPLC BEH C18 Column (1.7 µm × 2.1 mm × 150 mm, Waters, USA). Peptides were then analyzed by online nano flow liquid chromatography tandem mass spectrometry performed on an EASY-nLC 1200 (Thermo, USA) connected to a Orbitrap Exploris 480 (Thermo, USA) through a nano-electrospray ion source (Jia et al. 2018; Zhong et al. 2019). The raw data obtained from LC/LC–MS/MS were analyzed using Proteome Discoverer (Thermo Scientific, Version 2.4) against uniprot-taxonomy-133901. unique. fasta database. The false discovery rate (FDR) of peptide identification was set as FDR ≤ 0.01. Annotation of all identified proteins was performed using GO (<http://geneontology.org/>) and KEGG pathways (<http://www.genome.jp/kegg/>).

### Molecular cloning and bioinformatics analysis

Total RNA was extracted from male thrips using TRIzol (Invitrogen, Carlsbad, CA). The integrity, concentration, and purity of RNA were evaluated with a spectrophotometer (NanoDrop 2000c, MA, USA), and cDNA was synthesized using a reverse transcription kit (PrimeScript RT reagent Kit, Takara Biotech, Tokyo, Japan). Based on the transcriptome data of *F. occidentalis* in our laboratory, primers of *FoFSCB*-

*like* were designed with Primer3plus (Table 1). PCR reactions were performed using High-Fidelity Master Mix (Beijing Kinco Biotechnology Co. Ltd.) following the manufacturer's instructions. The 25 µL PCR reaction system contained 2 × High-Fidelity Master Mix 12.5 µL, forward and reverse primers (10 µmol/L) each 1 µL, cDNA template 1 µL, and nuclease-free water 9.5 µL. PCR reactions were performed as follows: 98°C 2 min; 98°C 10 s, 60°C 15 s, 72°C 50s, 35 cycles; 72°C 5 min (Wan et al. 2018). The amplified PCR product was sent to Sangon Biotech (Shanghai) Co., Ltd. for sequencing. SignalP (<http://www.cbs.dtu.dk/services/SignalP/>) and TMHMM (<http://www.cbs.dtu.dk/services/TMHMM/>) were used to predict signal peptide and the transmembrane domains, respectively. Protein conserved domains were identified using NCBI CDD Tools (<https://www.ncbi.nlm.nih.gov/cdd>). PROSITE(<https://prosite.expasy.org>), and Pfam (Pfam: [xfam.org](http://xfam.org)) was used to analyze the phosphorylation sites.

### qRT-PCR analysis

The expression profile of *FoFSCB-like* at different developmental stages of TSWV (+) and TSWV (-) groups was determined by qRT-PCR. Approximately 100 1<sup>st</sup>-instar nymphs, 100 2<sup>nd</sup>-instar nymphs, 80 pupae, 70 pupae, and 70 newly emerged male adults were collected. Total RNA extraction, cDNA synthesis, and primer design were conducted as described above. The reaction was performed in an ABI PRISM 7500 Real-time PCR System (Applied Biosystems, Foster City, CA, USA) with 20 µL, containing 2 × FastFire qPCR PreMix (SYBR Green) (Tiangen Biotech Co., Ltd., Beijing, China) 10 µL, cDNA template 1 µL, forward and reverse primers (10 pmol/µL) each 0.6 µL, 50 × ROX Reference Dye (Tiangen Biotech Co., Ltd., Beijing, China) 0.4 µL, and RNase-Free ddH<sub>2</sub>O 7.4 µL. The qRT-PCR program was as follows: 95°C 10 min (pre-denaturation); 95°C 15 s (denaturation), 60°C 30 s (annealing), 72°C 30 s (extension), 40 cycles (Peng et al. 2021). Succinate dehydrogenase (SDHA) (GenBank accession no. XM026420561.1) and β-actin (GenBank accession no. GQ290644) were selected as reference genes (Cifuentes et al. 2012), and the geometric means of the Ct values were used to normalize the target gene (Vandesompele et al. 2002). The relative expression level of *FoFSCB-like* was calculated using the 2<sup>-ΔΔCt</sup> method (Wan et al. 2018). Four biological and technical replicates were performed for each sample.

### Nanoparticle-mediated RNAi

Gene-specific dsRNA primers containing a T7 RNA polymerase promoter sequence (Table 1) were designed with the online dsRNA design tool ([https://www.flyrnai.org/cgi-bin/RNAi\\_find\\_primers.pl/](https://www.flyrnai.org/cgi-bin/RNAi_find_primers.pl/)). The T7 RiboMAX Express RNAi kit (Promega, Madison, WI, USA) was used to synthesize dsFoFSCB-like and dsEGFP according to the manufacturer's instructions. The integrity of the dsRNA was confirmed by 1.5 % agarose gel electrophoresis, and the dsRNA products were stored at -80°C. Because the expression of the *FoFSCB-like* gene was highest in pupae, pupae were used for subsequent RNAi. A nanoparticle-mediated RNAi method was performed as described by Peng et al. (2021), with some modifications. Approximately 70 pupae collected from the TSWV (-) group were placed in a disposable plastic petri dish (diameter = 3 cm). The dsRNA mixture (1 µg/µL of dsFoFSCB-like/dsEGFP and an equal volume of nanoparticles) were dripped onto pupae with a pipette. After 6 h, the treated pupae were transferred from the Petri dish to 1.5

mL centrifuge tubes for RNA extraction; control pupae were treated in the same manner except they were not exposed to the dsRNA. The interference efficiency was determined using qRT-PCR as described above. There were four biological replications for dsFoFSCB-like and dsEGFP treatments.

Approximately 40 pupae were treated with dsFoFSCB-like or dsEGFP. Newly emerged males were individually placed in a plastic cylinder (diameter = 8 cm, height = 6 cm) together with a healthy virgin female; a bean pod was provided for egg laying, and bean pods were collected and replaced every 2 days for a total of five collections. The bean pods with eggs that were collected each time were placed in a new plastic cylinder as described above and were reared in the usual way until adults emerged. The numbers of females and males were counted. At least 20 pairs (replications) were measured for each treatment.

### Statistical analysis

Unless otherwise stated, all quantitative data are presented as the means  $\pm$  SEM of at least three independent experiments. Differences ( $P < 0.05$ ) in relative gene expression among developmental stages were determined by one-way analysis of variance (ANOVA) with Tukey's HSD test (Graphpad Prism 8.0, San Diego, CA). Differences in relative gene expression, number of adults, and sex ratio between TSWV (+) and TSWV (-) groups, or between the dsEGFP and dsFoFSCB-like treatments, were determined using Student's *t*-test (Graphpad Prism 8.0, San Diego, CA).

## Results

### Effects of TSWV on the reproduction-related proteins

There were 104 differentially expressed proteins between the TSWV (-) group and the TSWV (+) group of *F. occidentalis*; among the 104 proteins, 67 were down-regulated and 37 up-regulated (Table S1). GO enrichment analysis was performed on the identified differential proteins in terms of biological process (BP), cellular component (CC), and molecular function (MF). The up-regulated proteins are shown in Fig. 1A, and the down-regulated proteins are shown in Fig. 1B. A total of 19 differentially expressed proteins were up-regulated in the BP category, 7 of which were enriched in cellular process and 6 in metabolic process. Among the 17 down-regulated differentially expressed proteins, 8 were enriched in cellular processes and 6 in metabolic processes. A total of 26 differentially expressed proteins were up-regulated and 17 were down-regulated in the CC category; these were mainly enriched in cellular anatomical entity. In the MF category, 27 differentially expressed proteins were up-regulated, which were mainly enriched in binding (13) and catalytic activity (10). The 49 differentially expressed proteins that were down-regulated were mainly enriched in binding (23), structural molecule activity (13), and catalytic activity (10).

The KEGG database was used for pathway analysis of the identified differentially expressed proteins (Fig. 2). The main pathways involved were metabolism, genetic information processing, environmental information processing, cellular process, organismal system, and human diseases. The up-regulated (Fig. 2A) and down-regulated (Fig. 2B) differentially expressed proteins were mainly enriched in two first-order pathways, human diseases and organismal system.

A total of 14 down-regulated proteins were related to spermatogenesis and sperm capacitation (Fig. 3). The expression of *FoFSCB-like*, a sperm-specific protein involved in sperm capacitation and motility, was significantly lower (by 46 %) in the TSWV (+) group than in the TSWV (-) group of *F. occidentalis* (Table S1).

### Structural features of *FoFSCB-like*

The full-length genomic DNA of the *FoFSCB-like* gene consisted of 2914 bp and contained six exons and five introns (Fig. 4A). The ORF of *FoFSCB-like* had 2478 bp that encoded 825 amino acid residues (Fig. 4B). The predicted *FoFSCB-like* included 10 Pro-X-X-Pro motifs, 8 N-myristoylation sites, 18 protein kinase C phosphorylation sites, 23 casein kinase II phosphorylation sites, 1 cAMP- and cAMP-dependent protein kinase phosphorylation site, 1 N-glycosylation site, and 1 amidation site (Fig. 4B). The theoretical isoelectric point of the *FoFSCB-like* protein was 5.93, its molecular weight was 86.8 kDa, and it included 104 negatively charged residues and 89 positively charged residues. Its instability index was 64.37, and its aliphatic index was 65.98. The protein was hydrophilic; its grand average of hydropathicity was -0.606 (Table 2).

### Temporal expression profiles of *FoFSCB-like* with and without TSWV

The expression level of *FoFSCB-like* was highest in pupae and lowest in nymphs (Fig. 5A). Relative to the expression level in the 1<sup>st</sup>-instar nymph (which had the lowest expression level), the *FoFSCB-like* expression level was 21.45, 58.64, and 11.14 times higher in pro-pupae, pupae, and adults, respectively (Fig. 5A). TSWV exposure significantly reduced *FoFSCB-like* expression in all developmental stages with the exception of pupae (Fig. 5E). The relative expression of *FoFSCB-like* in 1<sup>st</sup>-instar nymphs (Fig. 5B), 2<sup>nd</sup>-instar nymphs (Fig. 5C), pro-pupae (Fig. 5D), and adults (Fig. 5F) was 63.9 %, 48.3 %, 45.1 %, and 61.4 % lower, respectively, in the TSWV (+) group than in the TSWV (-) group.

### Functional characterization of *FoFSCB-like*

The expression level of *FoFSCB-like* in pupae was significantly decreased by 52 % after 6 h of interference (Fig. 6). Males were significantly more abundant than females among the offspring in the dsFoFSCB-like treatment, but females were significantly more abundant than males in the offspring of the control group (Fig. 7).

## Discussion

Although plant viruses are known to manipulate their insect vectors in order to increase virus transmission, the underlying molecular basis for these effects on vectors is largely unknown (Gilbertson et al. 2015; Oliver and Whitfield 2016).

### Differential proteins in proteomics of *F. occidentalis* with and without TSWV

Proteomics can be used to identify which proteins contribute to specific functions. Previous proteomic analyses of the 1st-instar nymphs of *F. occidentalis* demonstrated that 37 proteins were significantly altered in response to TSWV, 32 of which were likely associated with the infection cycle of other plant- and animal-infecting viruses and antiviral defense responses (Badillo-Vargas et al. 2012; Medeiros et al. 2004). In the current study, 104 proteins were found to be differentially expressed in male *F. occidentalis* with and without TSWV infection, and these proteins were related to nervous, endocrine, circulatory, and reproductive systems. Among the 104 proteins, 7 immune-related proteins were significantly up-regulated, including a lysosomal-associated organelle subunit WASH complex subunit 4, which may be involved in humoral immunity (Courtland et al. 2021). Ctenidin-3-like peptides rich in antimicrobial glycine and heat shock 70 kDa Protein II-like proteins may contribute to the defense against alien organisms and against biological and abiotic stresses (Baumann et al. 2010; Lyupina et al. 2014). Interestingly, 14 protein genes, including those encoding actin and E3 ubiquitin ligase (related to spermatogenesis), and calcium signal transduction protein, serine/threonine protein kinase, and FSCB-like protein (related to capacitation of sperm) were significantly down-regulated in males exposed to TSWV; sperm capacitation in particular may affect the function of *F. occidentalis* sperm. Actin is the skeleton protein formed by sperm cells (Ayscough and Winder 2004). MYO6, a myosin, regulates actin recombination in *Drosophila* sperm, and male *Drosophila* with this gene knocked out are sterile (Zakrzewski et al. 2021). In silkworm spermatogenesis, peristaltic squeezing of the spermatozoon strings, along with dynamic changes in actin, provides exogenous power for fertilization (Sahara and Kawamura 2004). Ubiquitination contributes to spermatogenesis via post-translational modification of proteins (Richburg et al. 2014). The degree of protein phosphorylation during sperm capacitation is related to the regulation of the protein kinase pathway. In mice in which the serine/threonine protein kinase GSK3a has been knocked out, sperm flagellum movement was abnormal and ATP levels were significantly reduced, resulting in male infertility (Bhattacharjee et al. 2015).

### Gene structure and function of FSCB

The fibrous sheath of the sperm flagellum is the main structure that ensures sperm motility, and its integrity is required for normal sperm function (Li et al. 2007). In *F. occidentalis* males infected with TSWV, a gene annotated as *FoFSCB-like* was significantly down-regulated by 46% (Table S1). When we cloned the whole genome and conducted conserved structure prediction and homology analysis, the results indicated that this gene shared the PXXP conserved motif with the *FSCB* gene reported in mammals, and shared similar phosphorylation sites with mice, including N-cardamylation sites, the protein kinase C phosphorylation site, the casein kinase II phosphorylation site, the camp-dependent protein kinase phosphorylation site, the N-glycosylation site, and others. However, no other shared conservative motifs were identified. Even the *FSCB* genes of rats, mice, and humans differ in size, conservative motifs, and phosphorylation sites. As is the case for arthropods in general, the sequence similarity between *F. occidentalis* and the above three mammals was even low, indicating that the *FSCB* gene differs substantially among species. The evolutionary relationships and function of the gene are also unknown and require further research. Among insects, *A. aegypti*, *D. melanogaster*, *B. dorsalis*,

*Armigera armigera*, *Plutella xylostella*, and *Spodoptera glabra* also have genes annotated as *FSCB*, but no further studies have been conducted. Therefore, the function of *FSCB* in insects needs further study.

*FSCB* is considered to be involved in sperm capacitation and is associated with sperm activity (Li et al. 2007; Liu et al. 2011; Zhang et al. 2016). In the current study, we investigated the role of *FoFSCB-like* in the reproduction of male *F. occidentalis*. We found that the expression of the *FoFSCB-like* gene was highest in the pupae and was significantly down-regulated in all *F. occidentalis* developmental stages infected with TSWV. We then used nanoparticle-mediated RNAi technology to interfere with the *FoFSCB-like* gene in male thrips and mated them with normal females. RNAi knockout of *FoFSCB-like* did not affect the total number of offspring but significantly increased the ratio of males to females. Male thrips develop from the haploid unfertilized egg, we infer that TSWV regulates the expression of *FoFSCB-like* and affects sperm capacitation during the reproductive process of male thrips, resulting in the failure of oocyte fertilization. As a consequence, the offspring sex ratio changed from female-biased to male-biased, indicating that *FoFSCB-like* helps explain how TSWV alters the sex ratio of *F. occidentalis* offspring.

## Effects Of Viruses On Sex Ratio Of Species

The sex ratio is a fundamental feature of all species with sexes and has profound effects on population dynamics (Bondy and Hunter 2019). Environmental change, such as poor host plant quality (Adam et al. 2017; Moreau et al. 2017), high temperature stress (Nigro et al. 2007), and lack of endosymbiotic bacteria (Wang et al. 2020) often leads to changes in insect sex ratios. Feeding on plants lacking a cytokinin receptor (irCHK2/3) increased the percentage of males in the offspring of the hemipteran *Tupiocoris notatus* (Adam et al. 2017). In Hymenoptera, an imbalance in the sex ratio can result from male sterility caused by high temperature or by different mortality rates between males and females (Nigro et al. 2007). The absence of endosymbiotic bacteria inhibits the fertilization of female whiteflies, resulting in the increase of haploid males in offspring and a male-biased sex ratio (Wang et al. 2020). By revealing why the sex ratio of *F. occidentalis* becomes male biased following exposure to TSWV, the results of the current study increase our understanding of the interactions between viruses and vectors. In the past, scientists have focused on females who produce offspring directly, such that research on sperm has been limited. In entomology, little research has been conducted on the effects of viruses on males. Because some infectious diseases tend to adversely affect the human reproductive system, research on the effects of viruses on males has focused on mammals. Zika virus is stored and replicates in the Leydig cells of testis. By inhibiting the expression of testosterone, the virus causes sperm damage and vas deferens destruction, which decreases fertility (Govero et al. 2016; Uraki et al. 2017). The outbreak of COVID-19 in 2019 has also been shown to affect the male reproductive system. Currently, SARS-CoV-2 is thought to cause gonadal dysfunction and to affect male reproduction via two mechanisms. On the one hand, the entry of SARS-CoV-2 into cells is mediated by the interaction between the viral spike protein (S) and the ACE2 protein of host cells, and ACE2 is highly expressed in Sertoli cells and Leydig cells in the

seminal tubules, suggesting that SARS-CoV-2 can cross the blood-testosterone barrier. On the other hand, SARS-CoV-2 affects male reproduction by limiting autophagy (Moshrefi et al. 2021).

### Potential applications of FoFSCB-like in SIT-based control of *F. occidentalis*

The population size and sex ratio of the host vector are important factors affecting the transmission of insect-borne pathogens. In addition to increasing the efficiency of virus transmission, the co-evolution of viruses and vector insects makes it easier for insects to feed and spread. In recent years, advances in molecular biology and omics technology have enabled researchers to better understand the interaction between vector insects and viruses and to consider new ways to control viruses and pests. With the SIT, certain pests can be controlled by releasing artificially sterile insects that interfere with the mating between fertile males and females. The release of sterile male mosquitoes into wild mosquito populations, for example, can reduce mosquito numbers and thereby reduce the transmission of mosquito-borne diseases such as Zika virus and yellow fever virus (Gato et al. 2021). Transgenic technology was recently used to insert dominant lethal genes into transposons of the codling moth *Cydia pomonella* in order to obtain sterile male moths and to thereby control populations below the economic threshold (Paterson et al. 2019). In the current study, we found that interference with the *FoFSCB-like* gene of *F. occidentalis* could cause male sterility. It follows that the induction of male sterility might be a useful way to control the *F. occidentalis*. For instance, by rearing and releasing sterile males in large numbers, they can mate with normal females to produce more male offspring. If the released number is large enough, the number of females in the population will be greatly reduced, which will reduce the population growth base and achieve the purpose of controlling *F. occidentalis*. The possibility warrants additional research.

## Declarations

### Author Contribution

MT, YW and QW conceived and designed research. MT conducted experiments. KQ, XZ and BX contributed new reagents and/or analytical tools. MT and YW analyzed data. MT and QW wrote the manuscript. YZ, XZ and QW revised the manuscript. All authors read and approved the manuscript.

**Funding:** This study was funded by China Agriculture Research System (CARS-24-C-02), the Natural Science Foundation of China (31572037), the Science and Technology Innovation Program of the Chinese Academy of Agricultural Sciences (CAAS-ASTIP-IVFCAAS), the China Postdoctoral Science Foundation (2020M670552).

### Compliance with ethical standards

**Conflict of interest** The authors declare that they have no conflict of interest.

**Human and animal rights** This article does not contain any studies with human participants or animals (vertebrates) performed by any of the authors.

**Informed consent** Informed consent was obtained from all individual participants included in the study.

## References

1. Adam N, Erler T, Kallenbach M, Kaltenpoth M, Kunert G, Baldwin IT, Schuman MC (2017) Sex ratio of mirid populations shifts in response to hostplant co-infestation or altered cytokinin signaling. *J Integr Plant Biol* 59: 44–59. <https://doi.org/10.1111/jipb.12507>
2. Akinyemi AO (2018) The copulation behaviour of the western flower thrips. Keele University, Keele.
3. Ayscough KR, Winder SJ (2004) Two billion years of actin. Meeting on cytoskeletal dynamics: from cell biology to developmental disease. *EMBO Rep* 5: 947–952. <https://doi.org/10.1038/sj.embo.7400252>
4. Baccetti B, Collodel G, Estenoz M, Manca D, Moretti E, Piomboni P (2005) Gene deletions in an infertile man with sperm fibrous sheath dysplasia. *Hum Reprod* 20: 2790–2794. <https://doi.org/10.1093/humrep/dei126>
5. Badillo-Vargas IE, Rotenberg D, Schnieweis DJ, Hiromasa Y, Tomich JM, Whitfield AE (2012) Proteomic analysis of *Frankliniella occidentalis* and differentially expressed proteins in response to *tomato spotted wilt virus* infection. *J Virol* 86: 8793–8809. <https://doi.org/10.1128/JVI.00285-12>
6. Baumann T, Kampfer U, Schurch S, Schaller J, Largiader C, Nentwig W, Kuhn-Nentwig L (2010) Ctenidins: antimicrobial glycine-rich peptides from the hemocytes of the spider *Cupiennius salei*. *Cell Mol Life Sci* 67: 2787–2798. <https://doi.org/10.1007/s00018-010-0364-0>
7. Bhattacharjee R, Goswami S, Dudiki T, Popkie AP, Phil CJ, Kline D, Vijayaraghavan S (2015) Targeted disruption of glycogen synthase kinase 3a (*Gsk3a*) in mice affects sperm motility resulting in male infertility. *Biol Reprod* 92: 65. <https://doi.org/10.1095/biolreprod.114.124495>
8. Blanc S, Michalakis Y (2016) Manipulation of hosts and vectors by plant viruses and impact of the environment. *Curr Opin Insect Sci* 16: 36–43. <https://doi.org/10.1016/j.cois.2016.05.007>
9. Bondy EC, Hunter MS (2019) Sex ratios in the haplodiploid herbivores, Aleyrodidae and Thysanoptera: A review and tools for study. *Adv Insect Physiol* 56: 251–281. <https://doi.org/10.1016/bs.aiip.2019.01.002>
10. Cifuentes D, Chynoweth R, Guillen J, De la Rua P, Bielza P (2012) Novel cytochrome P450 genes, CYP6EB1 and CYP6EC1, are over-expressed in acrinathrin-resistant *Frankliniella occidentalis* (Thysanoptera: Thripidae). *J Econ Entomol* 105: 1006–1018. <https://doi.org/10.1603/EC11335>
11. Courtland JL, Bradshaw TW, Waitt G, Soderblom EJ, Ho T, Rajab A, Vancini R, Kim IH, Soderling SH (2021) Genetic disruption of WASHC4 drives endo-lysosomal dysfunction and cognitive-movement impairments in mice and humans. *eLife* 10:e61590. <https://doi.org/10.7554/eLife.61590>
12. Fiedler SE, Dudiki T, Vijayaraghavan S, Carr DW (2013) Loss of R2D2 proteins ROPN1 and ROPN1L causes defects in murine sperm motility, phosphorylation, and fibrous sheath integrity. *Biol Reprod* 88: 41. <https://doi.org/10.1095/biolreprod.112.105262>

13. Fujita R, Inoue MN, Takamatsu T, Arai H, Nishino M, Abe N, Itokawa K, Nakai M, Urayama SI, Chiba Y, Amoa-Bosompem M, Kunimi Y (2020) Late male-killing viruses in *Homona magnanima* identified as Osugoroshi viruses, novel members of *Partitiviridae*. Front Microbiol 11: 620623.  
<https://doi.org/10.3389/fmicb.2020.620623>
14. Gato R, Menendez Z, Prieto E, Argiles R, Rodriguez M, Baldoquin W, Hernandez Y, Perez D, Anaya J, Fuentes I, Lorenzo C, Gonzalez K, Campo Y, Bouyer J (2021) Sterile Insect Technique: Successful suppression of an *Aedes aegypti* field population in Cuba. Insects 12: 469.  
<https://doi.org/10.3390/insects12050469>
15. Ghosh A, Priti, Mandal B, Dietzgen RG (2021) Progression of Watermelon Bud Necrosis Virus infection in its vector, *Thrips palmi*. Cells 10: 392. <https://doi.org/10.3390/cells10020392>
16. Gilbertson RL, Batuman O, Webster CG, Adkins S (2015) Role of the insect supervectors *Bemisia tabaci* and *Frankliniella occidentalis* in the emergence and global spread of plant viruses. Annu Rev Virol 2: 67–93. <https://doi.org/10.1146/annurev-virology-031413-085410>
17. Govero J, Esakky P, Scheaffer SM, Fernandez E, Drury A, Platt DJ, Gorman MJ, Richner JM, Caine EA, Salazar V, Moley KH, Diamond MS (2016) Zika virus infection damages the testes in mice. Nature 540: 438–442. <https://doi.org/10.1038/nature20556>
18. Jia J, Liu X, Li L, Lei C, Dong Y, Wu G, Hu G (2018) Transcriptional and translational relationship in environmental stress: RNAseq and iTRAQ proteomic analysis between sexually reproducing and parthenogenetic females in *Moina micrura*. Front Physiol 9: 812.  
<https://doi.org/10.3389/fphys.2018.00812>
19. Krueger S, Moritz G (2021) Sperm ultrastructure in arrhenotokous and thelytokous Thysanoptera. Arthropod Struct Dev 64: 101084. <https://doi.org/10.1016/j.asd.2021.101084>
20. Lehti MS, Sironen A (2016) Formation and function of the manchette and flagellum during spermatogenesis. Reproduction 151: R43-54. <https://doi.org/10.1530/REP-15-0310>
21. Li YF, He W, Jha KN, Klotz K, Kim YH, Mandal A, Pulido S, Digilio L, Flickinger CJ, Herr JC (2007) FSCB, a novel protein kinase A-phosphorylated calcium-binding protein, is a CABYR-binding partner involved in late steps of fibrous sheath biogenesis. J Biol Chem 282: 34104–34119.  
<https://doi.org/10.1074/jbc.M702238200>
22. Li YF, He W, Kim YH, Mandal A, Digilio L, Klotz K, Flickinger CJ, Herr JC (2010) CABYR isoforms expressed in late steps of spermiogenesis bind with AKAPs and ropporin in mouse sperm fibrous sheath. Reprod Biol Endocrinol 8: 101. <http://www.rbej.com/content/8/1/101>
23. Li YF, He W, Mandal A, Kim YH, Digilio L, Klotz K, Flickinger CJ, Herr JC, Herr JC (2011) CABYR binds to AKAP3 and Ropporin in the human sperm fibrous sheath. Asian J Androl 13: 266–274.  
<https://doi.org/10.1038/aja.2010.149>
24. Liu SL, Ni B, Wang XW, Huo WQ, Zhang J, Tian ZQ, Huang ZM, Tian Y, Tang J, Zheng YH, Jin FS, Li YF (2011) FSCB phosphorylation in mouse spermatozoa capacitation. BMB Rep 44, 541–546.  
<https://doi.org/10.5483/bmbrep.2011.44.8.541>

25. Lyupina YV, Orlova OV, Abaturova SB, Beljelarskaya SN, Lavrov AN, Mikhailov VS (2014) Egress of budded virions of *Autographa californica* nucleopolyhedrovirus does not require activity of *Spodoptera frugiperda* HSP/HSC70 chaperones. *Virus Res* 192: 1–5.  
<https://doi.org/10.1016/j.virusres.2014.08.002>
26. Ma ZZ, Zheng Y, Chao ZJ, Chen HT, Zhang YH, Yin MZ, Shen J, Yan S (2022) Visualization of the process of a nanocarrier-mediated gene delivery: stabilization, endocytosis and endosomal escape of genes for intracellular spreading. *J Nanobiotechnology* 20: 124. <https://doi.org/10.1186/s12951-022-01336-6>
27. Medeiros RB, Resende Rde O, de Avila AC (2004) The plant virus *Tomato Spotted Wilt Tospovirus* activates the immune system of its main insect vector, *Frankliniella occidentalis*. *J Virol* 78: 4976–4982. <https://doi.org/10.1128/JVI.78.10.4976-4982.2004>
28. Miki K, Willis WD, Brown PR, Goulding EH, Fulcher KD, Eddy EM (2002) Targeted disruption of the Akap4 gene causes defects in sperm flagellum and motility. *Dev Biol* 248: 331–342.  
<https://doi.org/10.1006/dbio.2002.0728>
29. Moreau G, Eveleigh ES, Lucarotti CJ, Morin B, Quiring DT (2017) Opposing effects of mortality factors on progeny operational sex ratio may thwart adaptive manipulation of primary sex ratio. *Ecol Evol* 7: 4973–4981. <https://doi.org/10.1002/ece3.3071>
30. Moshrefi M, Ghasemi-Esmailabad S, Ali J, Findikli N, Mangoli E, Khalili MA (2021) The probable destructive mechanisms behind COVID-19 on male reproduction system and fertility. *J Assist Reprod Genet* 38: 1691–1708. <https://doi.org/10.1007/s10815-021-02097-1>
31. Nakamura N, Dai Q, Williams J, Goulding EH, Willis WD, Brown PR, Eddy EM (2013) Disruption of a spermatogenic cell-specific mouse enolase 4 (eno4) gene causes sperm structural defects and male infertility. *Biol Reprod* 88: 90. <https://doi.org/10.1095/biolreprod.112.107128>
32. Nigro RG, Campos MCC, Perondini ALP (2007) Temperature and the progeny sex-ratio in *Sciara ocellaris* (Diptera, Sciaridae). *Genet Mol Biol* 30: 152–158. <https://doi.org/10.1590/S1415-47572007000100026>
33. Ogada PA, Moualeu DP, Poehling HM (2016) Predictive models for *Tomato Spotted Wilt Virus* spread dynamics, considering *Frankliniella occidentalis* specific life processes as influenced by the virus. *PLoS One* 11: e0154533. <https://doi.org/10.1371/journal.pone.0154533>
34. Oliver JE, Whitfield AE (2016) The genus Tospovirus: emerging Bunyaviruses that threaten food security. *Annu Rev Virol* 3: 101–124. <https://doi.org/10.1146/ANNUREV-VIROLOGY-100114-055036>
35. Paterson G, Perry GLW, Walker JTS, Suckling DM (2019) Peri-Urban Community Attitudes towards codling moth trapping and suppression using the Sterile Insect Technique in New Zealand. *Insects* 10:335. <https://doi.org/10.3390/insects10100335>
36. Plá I, de Oteyza JG, Tur C, Martínez MÁ, Laurín MC, Alonso E, Martínez M, Martín Á, Sanchis R, Navarro MC, Navarro MT, Argilés R, Briasco M, Dembilio Ó, Dalmau V (2021) Sterile insect technique programme against Mediterranean Fruit Fly in the valencian community (Spain). *Insects* 12: 415. <https://doi.org/10.3390/insects12050415>

37. Peng ZK, Ren J, Su Q, Zeng Y, Tian LX, Wang S, Wu QJ, Liang P, Xie W, Zhang YJ (2021) Genome-wide identification and analysis of chitinase-like gene family in *Bemisia tabaci* (Hemiptera: Aleyrodidae). *Insects* 12: 254. <https://doi.org/10.3390/insects12030254>
38. Richburg JH, Myers JL, Bratton SB (2014) The role of E3 ligases in the ubiquitin-dependent regulation of spermatogenesis. *Semin Cell Dev Biol* 30: 27–35. <https://doi.org/10.1016/j.semcd.2014.03.001>
39. Riley DG, Joseph SV, Srinivasan R, Diffie Stanley (2011) Thrips vectors of tospoviruses. *J. Integ. Pest Mngmt* 1: 2011. <https://doi.org/10.1603/IPM10020>
40. Rotenberg D, Jacobson AL, Schnieweis DJ, Whitfield AE (2015) Thrips transmission of tospoviruses. *Curr Opin Virol* 15: 80–89. <https://doi.org/10.1016/j.coviro.2015.08.003>
41. Sahara K, Kawamura N (2004) Roles of actin networks in peristaltic squeezing of sperm bundles in *Bombyx mori*. *J Morphol* 259: 1–6. <http://hdl.handle.net/2115/889>
42. Scholthof KB, Adkins S, Czosnek H, Palukaitis P, Jacquot E, Hohn T, Hohn B, Saunders K, Candresse T, Ahlquist P, Hemenway C, Foster GD (2011) Top 10 plant viruses in molecular plant pathology. *Mol Plant Pathol* 12: 938–954. <https://doi.org/10.1111/j.1364-3703.2011.00752.x>
43. Stafford CA, Walker GP, Ullman DE (2011) Infection with a plant virus modifies vector feeding behavior. *Proc Natl Acad Sci U S A* 108: 9350–9355. <https://doi.org/10.1073/pnas.1100773108>
44. Torres-Badia M, Solar-Malaga S, Martin-Hidalgo D, Hurtado de Llera A, Gomez-Candelo A, Garcia-Marin LJ, Gonzalez-Fernandez L, Bragado MJ (2021) Impaired mammalian sperm function and lower phosphorylation signaling caused by the herbicide Roundup Ultra Plus are due to its surfactant component. *Theriogenology* 172: 55–66. <https://doi.org/10.1016/j.theriogenology.2021.05.026>
45. Uraki R, Hwang J, Jurado KA, Householder S, Yockey LJ, Hastings AK, Homer RJ, Iwasaki A, Fikrig E (2017) Zika virus causes testicular atrophy. *Sci Adv* 3: e1602899. <https://doi.org/10.1126/sciadv.1602899>
46. Vandesompele J, De Preter K, Pattyn F, Poppe B, Van Roy N, De Paepe A, Speleman F (2002) Accurate normalization of real-time quantitative RT-PCR data by geometric averaging of multiple internal control genes. *Genome Biol* 3: RESEARCH0034.1-0034.11. <http://genomebiology.com/2002/3/7/research/0034.1>
47. Wan YR, Hussain S, Merchant A, Xu BY, Xie W, Wang SL, Zhang YJ, Zhou XG, Wu QJ (2020a) Tomato spotted wilt orthotospovirus influences the reproduction of its insect vector, western flower thrips, *Frankliniella occidentalis*, to facilitate transmission. *Pest Manag Sci* 76: 2406–2414. <https://doi.org/10.1002/ps.5779>
48. Wan YR, Yuan GD, He BQ, Xu BY, Xie W, Wang SL, Zhang YJ, Wu QJ, Zhou XG (2018) *Focca6*, a truncated nAChR subunit, positively correlates with spinosad resistance in the western flower thrips, *Frankliniella occidentalis* (Pergande). *Insect Biochem Mol Biol* 9: 1–10. <https://doi.org/10.1016/j.ibmb.2018.05.002>
49. Wan YR, Zheng XB, Xu BY, Xie W, Wang SL, Zhang YJ, Zhou XG, Wu QJ (2020b) Insecticide resistance increases the vector competence: a case study in *Frankliniella occidentalis*. *Journal of Pest Science*

- 94: 83–91. <https://doi.org/10.1007/s10340-020-01207-9>
50. Wang F, Fang Q, Wang BB, Yan ZC, Hong J, Bao YM, Kuhn JH, Werren JH, Song QS, Ye GY (2017) A novel negative-stranded RNA virus mediates sex ratio in its parasitoid host. *PLoS Pathog* 13: e1006201. <https://doi.org/10.1371/journal.ppat.1006201>
51. Wang YB, Ren FR, Yao YL, Sun X, Walling LL, Li NN, Bai B, Bao XY, Xu XR, Luan JB (2020) Intracellular symbionts drive sex ratio in the whitefly by facilitating fertilization and provisioning of B vitamins. *ISME J* 14: 2923–2935. <https://doi.org/10.1038/s41396-020-0717-0>
52. Wei J, He YZ, Guo Q, Guo T, Liu YQ, Zhou XP, Liu SS, Wang XW (2017) Vector development and vitellogenin determine the transovarial transmission of begomoviruses. *Proc Natl Acad Sci U S A* 114: 6746–6751. <https://doi.org/10.1073/pnas.1701720114>
53. Whitfield AE, Falk BW, Rotenberg D (2015) Insect vector-mediated transmission of plant viruses. *Virology* 479–480: 278–289. <https://doi.org/10.1016/j.virol.2015.03.026>
54. Xu KB, Yang LL, Zhang L, Qi HY (2020) Lack of AKAP3 disrupts integrity of the subcellular structure and proteome of mouse sperm and causes male sterility. *Development* 147: dev181057. <https://doi.org/10.1242/dev.181057>
55. Yan S, Ren BY, Shen J (2021) Nanoparticle-mediated double-stranded RNA delivery system: A promising approach for sustainable pest management. *Insect Science* 28: 21–34. <https://doi.org/10.1111/1744-7917.12822>
56. Young SAM, Miyata H, Satouh Y, Aitken RJ, Baker MA, Ikawa M (2016) CABYR is essential for fibrous sheath integrity and progressive motility in mouse spermatozoa. *J Cell Sci* 129: 4379–4387. <https://doi.org/10.1242/jcs.193151>
57. Yu XZ, Jia DS, Wang Z, Li GJ, Chen MN, Liang QF, Zhou YY, Liu H, Xiao M, Li ST, Chen Q, Chen HY, Wei TY (2021) A plant reovirus hijacks endoplasmic reticulum-associated degradation machinery to promote efficient viral transmission by its planthopper vector under high temperature conditions. *PLoS Pathog* 17: e1009347. <https://doi.org/10.1371/journal.ppat.1009347>
58. Zakrzewski P, Lenartowska M, Buss F (2021) Diverse functions of myosin VI in spermiogenesis. *Histochem Cell Biol* 155: 323–340. <https://doi.org/10.1007/s00418-020-01954-x>
59. Zhang T, Reitz SR, Wang HH, Lei ZR (2015) Sublethal effects of *Beauveria bassiana* (Ascomycota: Hypocreales) on life table parameters of *Frankliniella occidentalis* (Thysanoptera: Thripidae). *J Econ Entomol* 108: 975–985. <https://doi.org/10.1093/jee/tov091>
60. Zhang XQ, Chen MR, Yu RY, Liu BL, Tian ZQ, Liu SL (2016) FSCB phosphorylation regulates mouse spermatozoa capacitation through suppressing SUMOylation of ROPN1/ROPN1L. *Am J Transl Res* 8: 2776–2782. <https://www.ajtr.org/ISSN:1943-8141/AJTR0020298>
61. Zheng XY, Zhang DJ, Li YJ, Yang C, Wu Y, Liang X, Liang YK, Pan XL, Hu LC, Sun Q, Wang XH, Wei YY, Zhu J, Wei Q, Yan ZQ, Parker AG, Gilles JRL, Bourtzis K, Bouyer J, Tang MX, Zheng B, Yu JS, Liu JL, Zhuang JJ, Hu ZG, Zhang MC, Gong JT, Hong XY, Zhang ZB, Lin LF, Liu QY, Hu ZY, Wu ZD, Baton AB, Hoffmann AA, Xi ZY (2019) Incompatible and sterile insect techniques combined eliminate mosquitoes. *Nature* 572: 56–61. <https://doi.org/10.1038/s41586-019-1407-9>

62. Zhong Q, Wang B, Wang J, Liu Y, Fang X, Liao Z (2019) Global proteomic analysis of the resuscitation state of *Vibrio parahaemolyticus* compared with the normal and viable but non-culturable state. Front Microbiol 10: 1045. <https://doi.org/10.3389/fmicb.2019.01045>
63. Ziegler-Graff V (2020) Molecular insights into host and vector manipulation by plant viruses. Viruses 12: 263. <https://doi.org/10.3390/v12030263>

## Tables

**Table 1. Primers used in the study**

Primer	Primer sequence (5'-3')	Purpose
FoFSCB-like-F	CGCCATGAGGTTCAACAAACG	RT-PCR
FoFSCB-like-R	TCACGGGGCTCTTGAAAG	
qFoFSCB-like-F	CCAACCCCACAGCAGAGAC	RT-qPCR
qFoFSCB-like-R	CTGCGGTACCGACCTGAATT	
β-actin-F	CGGTCAAGTCATCACCATTG	
β-actin-R	TCGTCTCGTGTATTCCGCAC	
SDHA-F	GCGAAGTATCTTAGCACCAT	
SDHA-R	ATGCCCATCACCTCAGTTT	
dsFoFSCB-like-F	TAATACGACTCACTATAGGGAGACCAAAGAGAAGCAGGTAGCG	RNAi
dsFoFSCB-like-R	TCTCCCTATAGTGAGTCGTATTAGTTGTGTGTTCAATGCCG	

**Table 2. Characteristics of the *FoFSCB-like* protein.**

Characteristic	Description
Isoelectric point	5.93
Molecular weight	86.81 kDa
Total number of negatively charged residues	104
Total number of positively charged residues	89
Instability index	64.37
Aliphatic index	65.98
Grand average of hydropathicity	-0.606

# Figures

## Figure 1

GO enrichment analysis of differentially expressed proteins in male *F. occidentalis* with and without TSWV infection. A: GO enrichment analysis of up-regulated differentially expressed proteins; B: GO enrichment analysis of down-regulated differentially expressed proteins.

## Figure 2

KEGG enrichment analysis of differentially expressed proteins in male *F. occidentalis* with and without TSWV infection. A: KEGG enrichment analysis of up-regulated differentially expressed proteins; B: KEGG enrichment analysis of down-regulated differentially expressed proteins.

## Figure 3

The down-regulated proteins involved in sperm capacitation and spermatogenesis in male *F. occidentalis* infected with TSWV.

## Figure 4

**Basic gene information of *FoFSCB-like* in *F. occidentalis*.** A: Gene structure of *FoFSCB-like*. Orange boxes represent exons, and black lines represent introns. B: The nucleotide and amino acid sequence of *FoFSCB-like*.

Shown above is the open reading frame of the cDNA sequence and below is the amino acid sequence. The start and stop codons are double-underlined. The dark shade indicates the PXXP conservative motif; the light shade indicates the phosphorylation site of protein kinase C; italics indicate the N-myristoylation sites; and bold indicate the phosphorylation sites of casein kinase II. The box indicates the N-glycosylation site, the oval indicates the amidation site, and the single underline indicates the phosphorylation site of cAMP- and cGMP-dependent protein kinase.

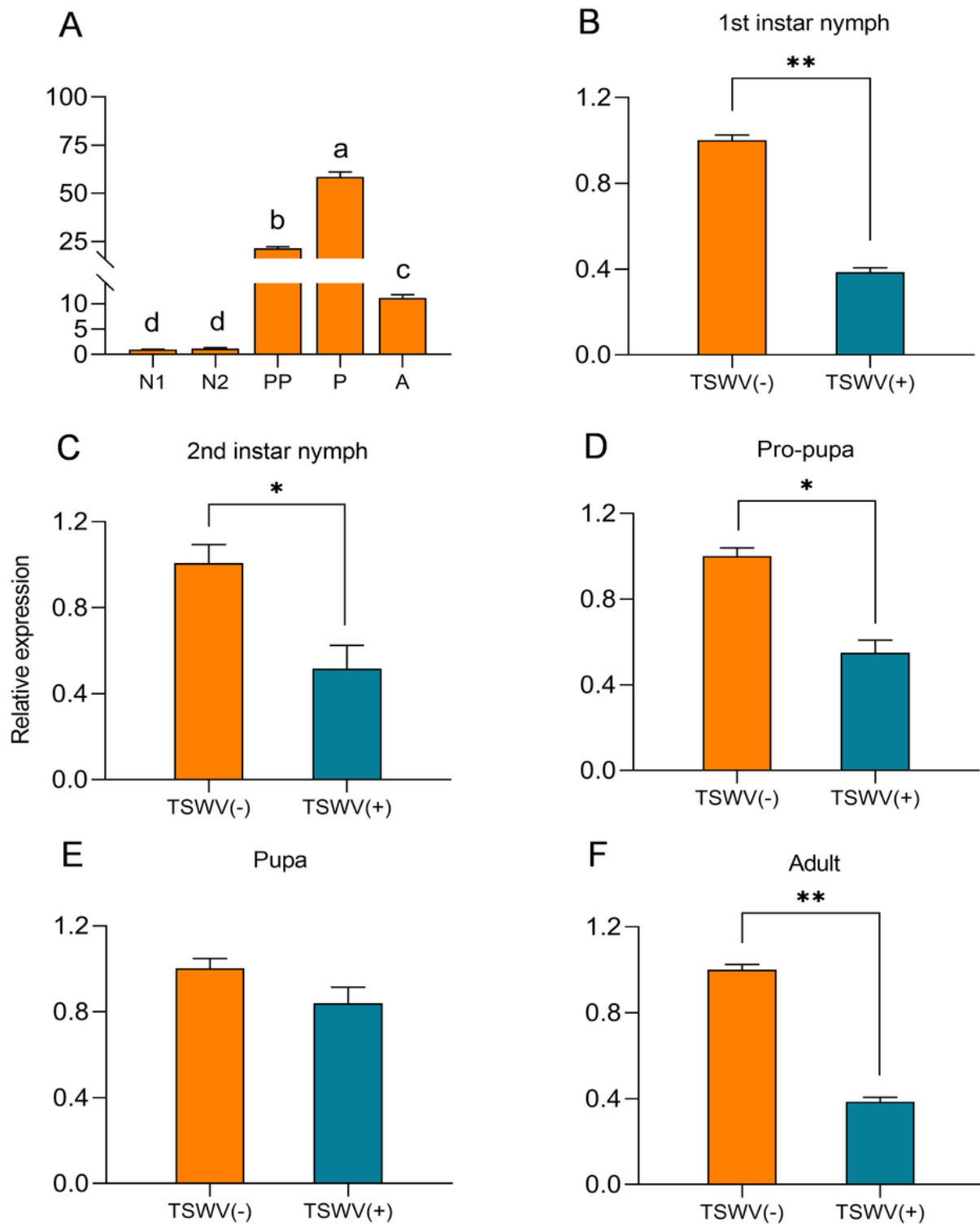


Figure 5

Expression profiles of *FoFSCB-like* in developmental stages of male *F. occidentalis* and effects of TSWV infection on *FoFSCB-like* expression. A: Relative expression of *FoFSCB-like* in developmental stages of male *F. occidentalis* without TSWV exposure. Relative expression (fold) was calculated based on the value of the lowest expression, which was detected in the 1<sup>st</sup>-instar nymph and which was assigned a value of 1. N1, 1<sup>st</sup>-instar nymph; N2, 2<sup>nd</sup>-instar nymph; PP, pro-pupa; P, pupa; and A, adult. B to F: *FoFSCB-like*

*like* expression levels in developmental stages of male thrips whose stage was exposed or not exposed to TSWV. Relative expression (fold) was calculated based on the expression of the TSWV (-) group, which was assigned a value of 1.

TSWV (-), thrips without TSWV infection; TSWV (+), thrips with TSWV infection. Values are means  $\pm$  SEM of at least three biological replicates.  $*p < 0.05$ ,  $**p < 0.01$ .

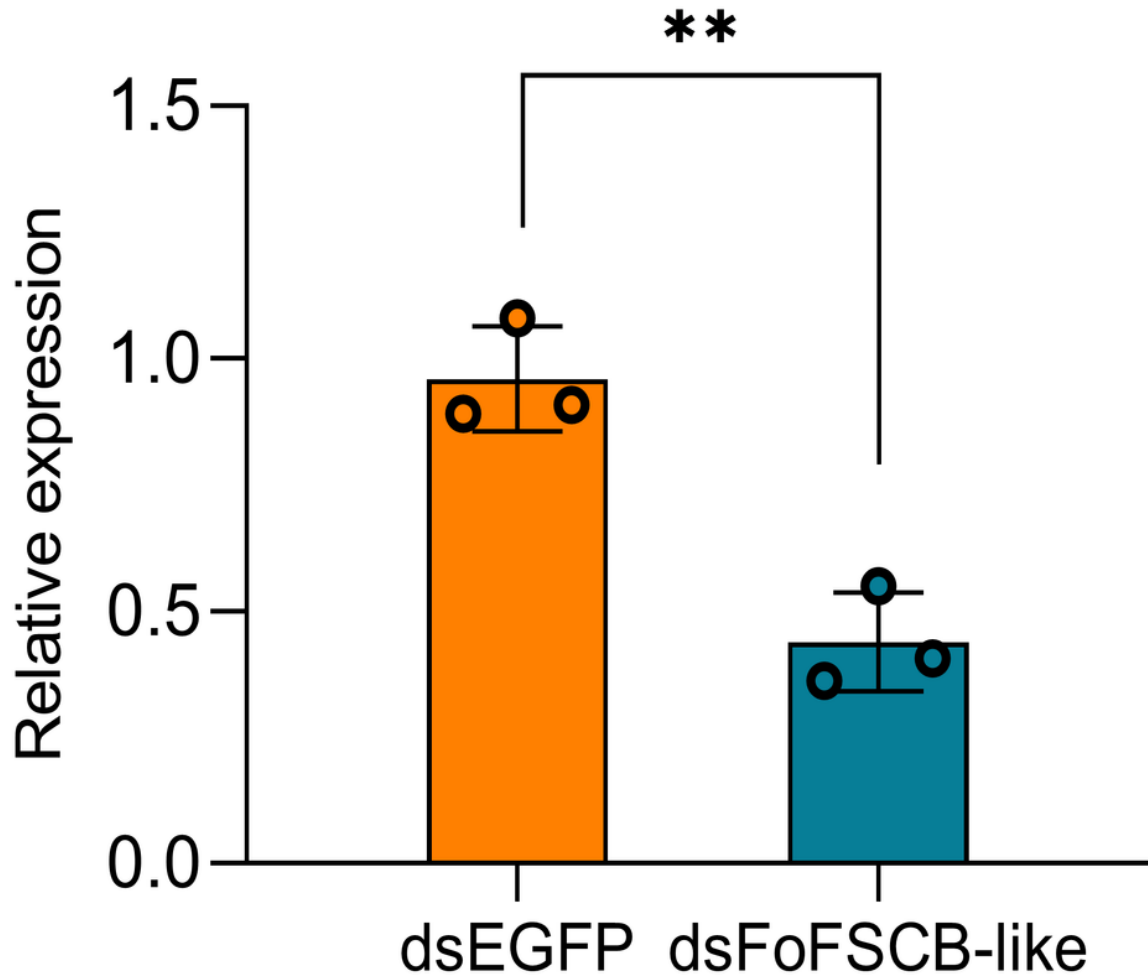
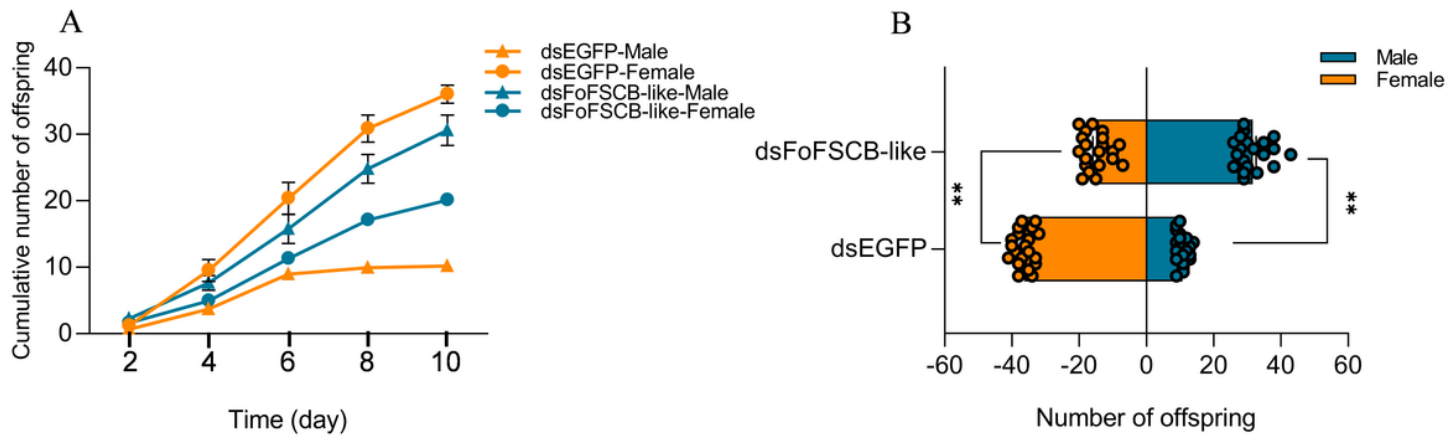


Figure 6

Relative expression level of *FoFSCB-like* after 6 h of interference at the pupal stage.

Values are means  $\pm$  SEM of at least three biological replicates.  $**p < 0.01$ .



**Figure 7**

Effects of *FoFSCB-like* gene silencing on the number of female and male offspring. A: Cumulative number of female and male offspring produced per female every 2 days. B: Total number of female and male offspring produced per female over a 10-day period.

Values are means  $\pm$  SEM of at least 20 biological replicates. \*\* $p < 0.01$ .

## Supplementary Files

This is a list of supplementary files associated with this preprint. Click to download.

- [Supportinginformation.docx](#)